*Nonlinear Dynamics* **6:** 101–124, 1994.


# Melnikov Analysis for a Ship with a General Roll-Damping Model

M. BIKDASH[1], B. BALACHANDRAN[2], and A. NAYFEH[2]
[1] *Bradley Department of Electrical Engineering,* [2] *Department of Engineering Science and Mechanics, Virginia Polytechnic Institute and State University, Blacksburg, VA 24061-0219, U.S.A.*

(Received: 9 July 1992; accepted: 8 February 1993)

**Abstract.** In the framework of a general roll-damping model, we study the influence of different damping models on the nonlinear roll dynamics of ships through a detailed Melnikov analysis. We introduce the concept of the Melnikov equivalent damping and use phase-plane concepts to obtain simple expressions for what we call the Melnikov damping coefficients. We also study the sensitivity of these coefficients to parameter variations. As an application, we consider the equivalence of the linear-plus-cubic and linear-plus-quadratic damping models, and we derive a condition under which the two models yields the same Melnikov predictions. The free- and forced-oscillation behaviors of the models satisfying this condition are also compared.

**Key words:** Melnikov criterion, Duffing equation, ship dynamics, damping models.

## 1. Introduction

Ship-roll motions are of paramount importance for determining the conditions under which a ship can experience dynamic capsizing. Although capsizing is a dynamic phenomenon, the traditional (and empirical) ship stability criteria are based only on nonlinear hydrostatics. Traditionally, the righting arm is plotted against the roll angle, and the characteristics of this curve (the GZ curve) are examined to see if they meet the requirements based on empirical criteria (the IMCO Stability Criteria). Although roll damping has been recognized to be crucial for assessing ship stability since the days of Froude [1], the dynamic effect of different damping mechanisms has not been taken into account in the formulation of ship stability criteria. Furthermore, the equations of motion are linearized in traditional ship-motion analysis. The work presented in many recent studies (e.g. [2–11]) has brought out the importance of considering nonlinear dynamics for determining ship stability.

Wright and Marshfield [2] conducted an interesting analytical and experimental study of nonlinear ship-rol motions. One of the ship models treated in their study will be used as an example in our study. Nayfey and Khdeir [3] used a second-order perturbation analysis and presented analytical and numerical results to illustrate different types of nonlinear motions. Continuing the work presented in [3], Nayfeh and Sanchez [4, 5] conducted a local-global study with the aid of digital and analog computers and provided results in the form of response curves, bifurcation sets, and basins of safe and capsize regions. They addressed the different routes through which capsizing is likely to occur in regular beam seas. A quintic polynomial was used to approximate the restoring terms in [3–5]. Nayfeh and Sanchez [4, 5] investigated dynamic capsizing in the context of both transient and steady-state motions. Virgin [6] conducted a numerical study to examine capsizing in regular beam seas.

Falzarano and Troesch [9] and Falzarano [10] applied geometric concepts of nonlinear dynamics to study the dynamic response of different vessels, and studied the invariant manifolds of the Poincaré map [12] to examine the nature of the boundaries between safe and capsize regions. Falzarano [10] discussed in detail the derivation of the equations of motion of many ship models and the physical meaning of different restoring and damping terms. Moreover, the applicability of the Melnikov analysis and of lobe dynamics to ship problems was advocated and illustrated. Falzarano *et al.* [11] modeled the roll motion by a second-order differential equation with linear and quadratic damping terms and linear and cubic restoring terms. Using closed-form expressions of the heteroclinic and homoclinic manifolds of the underforced and undamped system, they were able to compute the corresponding Melnikov function in closed form, and consequently, to obtain closed-form expressions for the critical values of the forcing at which the homoclinic or heteroclinic bifurcations occur.

Thompson, Rainey and Soliman [7] examined dynamic capsizing in the context of transient motions. They used a model with linear and quadratic restoring terms and a linear damping term. More realistic models obtained from semi-empirical data with quadratic damping and quintic restoring terms were also considered [8].

Thompson *et al.* [7] examined the erosion of the basins of safe motions in regular beam seas and quantified basin erosion in the form of integrity diagrams; that is, diagrams that show variation of the area of the basin of safe motion as the forcing amplitude is varied. These integrity diagrams require a tremendous computational effort. The integrity diagrams in [7] show clearly that the area of the safe region is almost constant for all forcing amplitudes smaller than the maximum safe forcing amplitude predicted by the Melnikov analysis [12–15], but that this area decreases very rapidly as the forcing amplitude is increased beyond the maximum safe forcing amplitude. These integrity diagrams, as well as simulations conducted in [4, 5] using other ship models, also illustrate the importance of conducting a Melnikov analysis, at least for the case where the forcing is an external excitation.

We note however that in other cases, such as in the case of a parametric excitation [16], the rapid erosion of the safe region sometimes occurs at forcing levels that are significantly higher than the critical levels predicted by the Melnikov criterion, if at all. This behavior is related to the intersections of the invariant manifolds of the corresponding Poincaré map, and it is therefore a harder and more intricate problem. In any case, the Melnikov criterion may be regarded as an often-accurate, always-conservative predictor of rapid loss of safety.

Froude [1] proposed a damping model with linear and quadratic terms. Many other interesting studies on roll damping have also been conducted [17–21]. In [2–5], damping models with linear and cubic terms are used. Dalzell [17] developed the linear-plus-cubic damping (LPCD) model as an approximation to the linear-plus-quadratic damping (LPQD) model of Froude. This is motivated by the fact that the LPCD model, being infinitely differentiable, is mathematically preferable to the LPQD model, which is only once continuously differentiable. Dalzell proposed a procedure to approximate the LPQD model by a LPCD model by minimizing a square error term over a given finite range of roll velocities and suggested an iterative procedure to determine this range. The results of this procedure, however, depend on the forcing conditions, and hence, the procedure has to be repeated for different forcing conditions.

Cardo, Francescutto, and Nabergoj [18] used the method of averaging [23] to obtain approximate solutions of the roll equation. Because the form of the obtained approximate solutions was different for the LPQD and LPCD models, they concluded that the roll oscillations are sensitive to the form of the damping model. Mathisen and Price [19] considered damping

models in which the nonlinear part is weak in comparison to the linear part. They carried out straightforward perturbation analyses to study free and forced oscillations and showed that their analytical results agree with some experimental data. The equations in both references [18] and [19] contain only linear restoring terms.

Bass and Haddara [20] examined different roll-damping models used in literature and presented a scheme to determine the damping coefficients from free-decay data. The angle dependence of the roll-damping moment was examined in [20, 21]. The restoring roll moment used in reference [20] contains both linear and cubic terms. In [18–21], the focus was on the different damping models and the determination of damping coefficients. The influence of damping models on capsizing and complicated motions was not addressed in these studies. The work of Lugovsky [22] on ship motions should also be noted.

In this paper, we investigate the influence of a general roll-damping model on the stability of ships using the Melnikov criterion, and we compare and characterize the effect of different damping models. In Section 2, we discuss in some detail the ship model under consideration. In Section 3, we discuss the topology of the phase plane corresponding to the undamped and unforced part of our model. The Melnikov analysis, which we present and discuss in Section 4, is based upon this topology. In Section 4, we also introduce the concept of the Melnikov equivalent damping, and we show that it is independent of the forcing. In Section 5, we conduct a detailed analysis of a general damping model and compute, often in closed form, the Melnikov equivalent damping using the first integral of motion of the undamped and unforced system. As an application of our Melnikov analysis to different damping models, we consider in Section 6 the issue of approximating a linear-plus-quadratic damping model with a linear-plus-cubic model, and we propose an approximation procedure which is independent of the forcing (sea state).

## 2. Ship-Roll Motions in Regular Beam Seas

In this paper, we use a second-order nonautonomous system of equations to model ship-roll motions. We assume that the ship does not possess any forward speed and that the ship-roll motions are uncoupled from other motions. The latter assumption is not a good one in the presence of internal resonances (e.g., [24]). In the context of ship motions, an internal resonance can occur when the pitch frequency is about twice the roll frequency. This phenonemon is likely to occur in fishing vessels, where the pitch frequence is about 1.5 to 3 times the roll frequency [25]. The damping models used in this study are all assumed to be independent of the frequency of the roll oscillations. In this paper, the damping and periodic forcing terms are assumed to be weak; they are treated as first-order perturbations to the Hamiltonian part of the system under consideration. One may also be able to apply the Melnikov criterion to a system with a nonweak damping as illustrated in [15]. Unfortunately, the unperturbed system in this case, which is not Hamiltonian may not have a homoclinic or heteroclinic orbit. This makes the Melnikov criterion inapplicable.

Following Wright and Marshfield [2], we write the equation for rolling motions in terms of the relative roll angel $\phi$ as

$$(I + \delta I)\ddot{\phi} + \tilde{D}(\phi, \dot{\phi}) + K(\phi) = B - I\ddot{s}, \tag{1}$$

where $s$ is the wave slope, $I$ is the rotational moment of inertia, $\delta I$ is the added moment of inertia due to the surrounding fluid, the overdot denotes differentiation with respect to time $t$, and $B$ is a constant bias moment which might be due to a steady wind or an imbalance in

cargo loading. The roll-damping moment $\tilde{D}$ depends on many factors, such as the forward speed of the vessel, the vessel profile, antiroll fins, and bilge keels. We assume that $B = 0$ and $\delta I$ is constant.

The restoring moment $K(\phi)$ is approximated by an old polynomial of the form [3–5]

$$\frac{K(\phi)}{(I + \delta I)} \simeq \alpha_1 \phi + \alpha_3 \phi^3 + \alpha_5 \phi^5. \tag{2}$$

Because $B = 0$, the ship is unbiased and the upright position corresponds to an equilibrium. We assume that the coefficients in equation (2) are such that the potential energy of the system has a local minimum at $\phi = 0$, making it a stable equilibrium position. The form of the GZ curve is modified when there is water on deck, and the coefficients in equation (2) are such that there is an unstable equilibrium at the upright position and a stable equilibrium at the position corresponding to the angle of roll [9].

In regular beam seas, the wave slope can be written as $s(t) = s_m \cos(\Omega t)$, where $s_m$ is the maximum wave slope and $\Omega$ is the encounter frequency. Substituting equation (2) into equation (1) yields

$$\ddot{\phi} + D(\phi, \dot{\phi}) + \alpha_1 \phi + \alpha_3 \phi^3 + \alpha_5 \phi^5 = f \cos(\Omega t), \tag{3}$$

where $D(\phi, \dot{\phi}) = \tilde{D}(\phi, \dot{\phi})/(I + \delta I)$ and

$$f = \frac{I}{I + \delta I} s_m \Omega^2. \tag{4}$$

For the unbiased, low-freeboard ship model of Wright and marshfield [2], which is also used in [3–5], the coefficients in equations (3) and (4) have the following values:

$$\begin{aligned} &\omega_0 = 5.278, \quad \alpha_1 = \omega_0^2, \quad \alpha_3 = -1.402\omega_0^2, \\ &\alpha_5 = 0.271\omega_0^2, \quad \text{and} \quad \frac{I + \delta I}{I} = 1.25. \end{aligned} \tag{5}$$

In equation (5), $\omega_0$ is the linear natural roll frequency of the ship.

## 3. Topology of the Phase Plane

We begin by rewriting equation (3) in the form

$$\ddot{\phi} + \epsilon D(\phi, \dot{\phi}) + \alpha_1 \phi + \alpha_3 \phi^3 + \alpha_5 \phi^5 = \epsilon f \cos \Omega t, \tag{6}$$

where $\phi$ represents the roll angle, $D(\phi, \dot{\phi})$ is a general damping term, and $\epsilon$ is a small bookkeeping device artificially introduced to make explicit the terms that we consider to be small perturbations. Hence, we will set $\epsilon = 1$ in the final analysis. In equation (6), we assume the damping and forcing terms to be small.

Setting $\epsilon = 0$, we obtain the Hamiltonian system

$$\ddot{\phi} + \alpha_1 \phi + \alpha_3 \phi^3 + \alpha_5 \phi^5 = 0. \tag{7}$$

Defining $x_1 = \phi$ and $x_2 = \dot{\phi} = \psi$, we can write equation (6) in the state-space form

$$\dot{\mathbf{x}} = \mathbf{h}(\mathbf{x}) + \epsilon \mathbf{g}(\mathbf{x}, t; \text{ parameters}), \tag{8}$$

where $\mathbf{x} \in \mathbb{R}^2$ and $\mathbf{h}$ and $\mathbf{g}$ are $C^r$ (i.e., $r$ times continuously differentiable) with $r \geq 1$. We note that $\dot{\mathbf{x}} = \mathbf{h}(\mathbf{x})$ is a Hamiltonian system defined by

$$h_1 = x_2, \quad h_2 = -\alpha_1 x_1 - \alpha_3 x_1^3 - \alpha_5 x_1^5 \tag{9}$$

and $\epsilon \mathbf{g}(\mathbf{x}, t; .)$ is a small perturbation, not necessarily Hamiltonian, given by

$$g_1 = 0, \quad g_2 = -D(x_1, x_2) + f \cos \Omega t. \tag{10}$$

The equilibrium points of equation (7) satisfy the equation

$$\alpha_1 \phi_e + \alpha_3 \phi_e^3 + \alpha_5 \phi_e^5 = 0, \tag{11}$$

which admits the solutions

$$\phi_e = 0, \quad \phi_e^2 = \frac{-\alpha_3 \pm \sqrt{\alpha_3^2 - 4\alpha_1 \alpha_5}}{2\alpha_5}. \tag{12}$$

If $\alpha_3^2 - 4\alpha_1\alpha_5 < 0$, equation (11) admits only one real root which is the origin. Otherwise, there are either three or five real roots depending on the signs of the $\alpha_i$, as seen from equation (12).

EXAMPLE. In Figure 1a, we show a few trajectories in the phase plane of the Hamiltonian system given by equation (7) for the unbiased low-freeboard model of [2] defined by the parameters in equation (5), for which $\phi_e = 0, \pm 0.9243$, and $\pm 2.0783$. We let $\phi_s = 0.9243$ represents the saddle point the right-half of the phase plane.

For the unbiased low-freeboard ship of [2], which is representative of ships with cubic and quintic roll restoring terms, we can make the following statements. There is a center $C_0$ at $(\phi, \psi) = (0, 0)$ around which the ship rolls and two saddles $S_1$ at $(-\phi_s, 0)$ and $S_2$ at $(\phi_s, 0)$. The two saddles are connected through the two heteroclinic half-orbits $S_1P_1S_2$ and $S_2P_2S_1$. The half-orbit $S_1P_1S_2$ represents the unstable manifold of $S_1$ and the stable manifold of $S_2$. We refer to the union of $S_1P_1S_2$ and $S_2P_2S_1$ as the heteroclinic orbit $\Gamma_\infty$. The half-orbits are also called separatrices because they separate the basins of existence and/or attraction for qualitatively different solutions in the phase plane. For the unforced system, the region outside the heteroclinic orbit $\Gamma_\infty$ is "unsafe", while the region inside it is "potentially safe". We call a region "unsafe" (or a "capsize region"), if initial conditions in this region can lead to capsizing. The two centers at $(-2.0782, 0)$ and $(2.0782, 0)$ are enclosed by homoclinic orbits. However, they are not physically relevant, but are only of mathematical interest, because they correspond to roll angles that most probably result in vessel foundering. Within the heteroclinic orbit (and similarly, within the homoclinic orbits), there is a continuum of periodic solutions $\Gamma_1, \Gamma_2, \ldots$ with periods $T_1, T_2, \ldots$ with the property that $T_i \to \infty$ as $\Gamma_i \to \Gamma_\infty$.

In Figure 1b, we show the effect of adding damping. The heteroclinic orbit is destroyed, and the stable and unstable manifolds of the saddle points are now distinct.

A straightforward analysis (e.g., [23]) of equation (7) yields the following integral of motion:

$$\dot{\phi} = \psi(\phi) = \pm \sqrt{\psi_{\max}^2 - \left[\alpha_1 \phi^2 + \frac{1}{2}\alpha_3 \phi^4 + \frac{1}{3}\alpha_5 \phi^6\right]}, \tag{13}$$

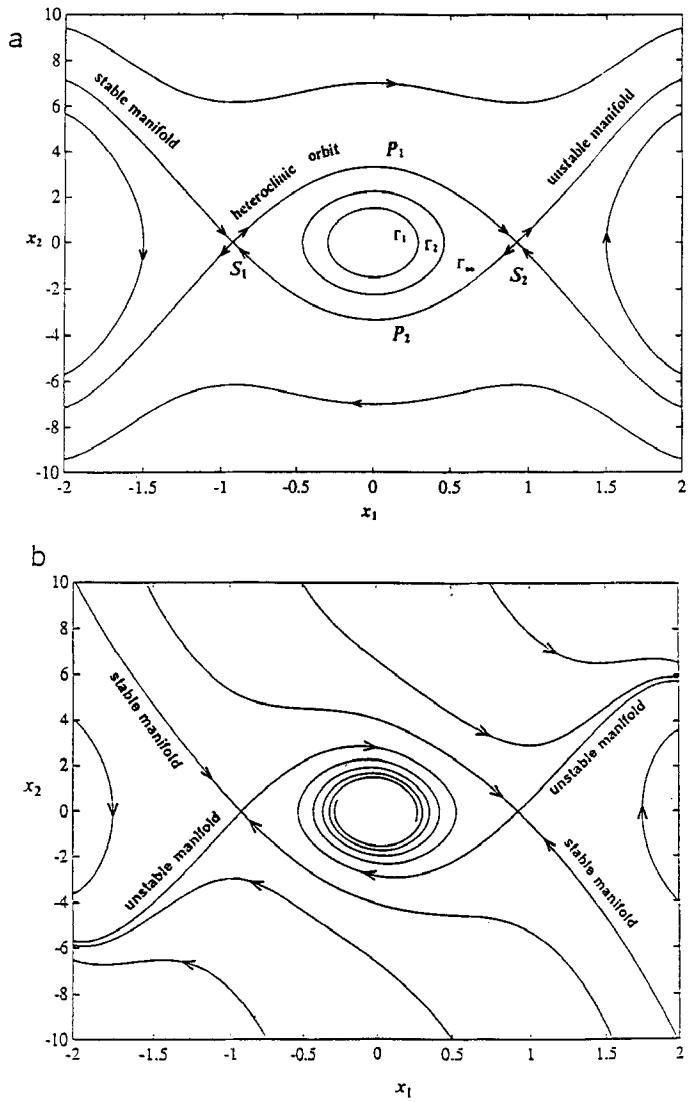


*Fig. 1.* (a) Phase portrait of the undamped and unforced Hamiltonian system and (b) Phase portrait of the damped and unforced system.

where $\psi_{\max}$ depends on the $\alpha_i$ and the initial conditions, and hence any specific trajectory in the phase plane can be obtained by a proper choice of $\psi_{\max}$. The heteroclinic half-orbits are determined by noting that at the saddle points $\pm\phi_s$ we have $\psi = 0$. Hence,

$$\psi_{\max}^2 = \alpha_1\phi_S^2 + \frac{1}{2}\alpha_3\phi_S^4 + \frac{1}{3}\alpha_5\phi_S^6. \tag{14}$$

For the parameters in equation (5), we have $\psi_{\max} = 3.334$ rad/sec.

If $\alpha_5 = 0$, equation (13) can be integrated using separation of variables, yielding a closed-form expression for the heteroclinic half-orbits. When $\alpha_5 \neq 0$, or for more general systems, the heteroclinic orbit can be computed by numerically integrating $\dot{\mathbf{x}} = \mathbf{h}(\mathbf{x})$ with the proper initial conditions $\mathbf{x}_0$ belonging to the heteroclinic orbit. Any point very close to the saddle point, but which is inside the heteroclinic orbit, is a reasonable choice. Discussions of more sophisticated techniques can be found in Parker and Chua [26]. Alternatively, we can also

solve the initial-value problem in equation (13) with the initial condition $\phi(0) = 0$ over the time interval $[0, \infty]$. Subsequently, even symmetry about the $\psi$ and $\phi$ axes can be used to complete the heteroclinic orbit. Finally, we note that the dependence of the saddle point $\phi_S$ on some parameter $\alpha_i$ is given by the differential equation

$$\frac{d\phi_S}{d\alpha_i} = -\frac{\phi_S^i}{\alpha_1 + 3\alpha_3\phi_S^2 + 5\alpha_5\phi_S^4}. \tag{15}$$

Most of the previous and subsequent analysis can be generalized to any Hamiltonian system $\mathbf{h}(\mathbf{x})$ having the polynomial form

$$\ddot{\phi} + \sum_{i=1}^{N} \alpha_i \phi^i = 0, \qquad h_1 = x_2, \qquad h_2 = -\sum_{i=1}^{N} \alpha_i x_1^i \tag{16}$$

and equations (13) and (15) become, respectively,

$$\dot{\phi} = \psi(\phi) = \pm\sqrt{\Psi(\phi_S) - \Psi(\phi)}, \qquad \Psi(\phi) = 2\sum_{i=1}^{N} \frac{\alpha_i}{i+1}\phi^{i+1} \tag{17}$$

and

$$\frac{d\phi_S}{d\alpha_i} = -\frac{\phi_S^i}{\sum_{j=1}^{N} j\alpha_j \phi_S^{j-1}}. \tag{18}$$

Equation (7) can be obtained from equation (16) by choosing $\alpha_2 = \alpha_4 = 0$ and $\alpha_i = 0$ for $i \geq 6$. The importance of equations (15) and (18) will become apparent in Section 5.3.

## 4. The Melnikov Criterion

The Melnikov analysis is a global analysis technique that yields a condition on the occurrence of a heteroclinic (or homoclinic) bifurcation. Such a bifurcation is said to have occurred if a heteroclinic (homoclinic) set is either created or destroyed as a parameter is varied. The occurrence of these bifurcations can lead to major changes in the basins of attraction of qualitatively different types of motion, the onset of chaos, and the mixing or intermingling between the safe and unsafe regions [12, 27]. The Melnikov criterion helps in an indirect way in ascertaining the values of the different parameters for which the heteroclinic or homoclinic bifurcations occur, and hence, for which the basins of safe and capsize regions are likely to be intermingled. This intermingling is not desirable in the context of capsizing. Furthermore, we consider an increase in the area of the safe region due to a parameter, such as damping, as a stabilizing effect.

The Melnikov analysis is based on the heteroclinic (homoclinic) orbits and can be computed once these state trajectories are known. To apply the Melnikov analysis, one assumes that the stable and unstable manifolds of the saddle points of the Poincaré map of equation (6), shown schematically in Figure 2, are perturbations of the stable and unstable manifolds of the saddle points of the suspended Hamiltonian system $\dot{\mathbf{x}}(t) = \mathbf{h}(\mathbf{x})$ and $\dot{\theta} = \Omega$, $\theta \in S^1$ with $\theta = \Omega t$ modulo $2\pi$. Melnikov [13] constructed a function, now known as the Melnikov function, that represents the signed distance between the stable and unstable manifolds or the saddle

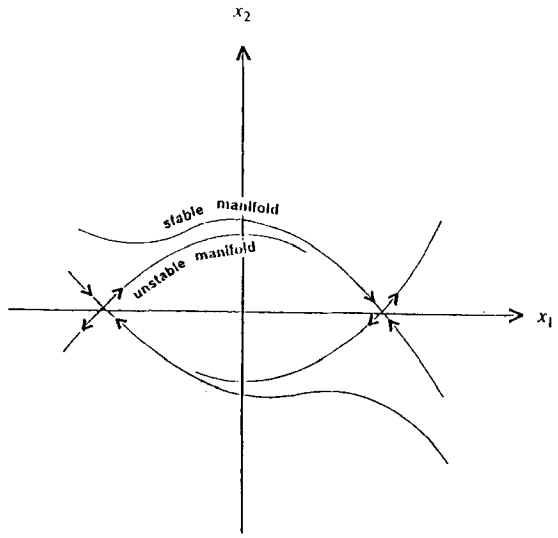


*Fig. 2.* A sketch of the manifolds of the saddle points on a Poincaré section of the perturbed system.

points of the Poincaré map associated with equation (6). When the unperturbed system is Hamiltonian, this function assumes the form

$$M(t_0;\ \text{parameters}) = \int_{-\infty}^{\infty} \mathbf{h}[\tilde{\mathbf{x}}(t)] \wedge \mathbf{g}[\tilde{\mathbf{x}}(t), t + t_0]\ \mathrm{d}t \tag{19}$$

where the wedge operator $\wedge$ is defined as

$$\mathbf{h} \wedge \mathbf{g} = h_1 g_2 - h_2 g_1 \tag{20}$$

and $\tilde{\mathbf{x}}(t) = (\tilde{x}_1(t), \tilde{x}_2(t))$ denotes the state trajectory along the heteroclinic upper half-orbit $S_1 P_1 S_2$. (More general forms of the Melnikov function can be found in [12, 15].)

To evaluate the Melnikov function, we substitute equations (9) and (10) into equation (19) and obtain

$$M(t_0, .) = -D_e + f(F_c\ \cos\Omega t_0 + F_s\ \sin\Omega t_0), \tag{21}$$

where $D_e$, which we call the Melnikov equivalent damping, is a measure of the effect of the general damping term and is given by

$$D_e = \int_{-\infty}^{\infty} \tilde{x}_s(t) D[\tilde{x}_1(t), \tilde{x}_2(t)]\ \mathrm{d}t \tag{22}$$

and

$$F_c(\Omega) = \int_{-\infty}^{\infty} \tilde{x}_2(t)\ \cos\Omega t\ \mathrm{d}t, \qquad F_s(\Omega) = -\int_{-\infty}^{\infty} \tilde{x}_2(t)\ \sin\Omega t\ \mathrm{d}t. \tag{23}$$

In Figure 3, we show the time histories of the states $\tilde{x}_1(t)$, $\tilde{x}_2(t)$, and $\tilde{x}_1(t)\tilde{x}_2(t)$. We note that $\tilde{x}_2(t)$ and $\tilde{x}_1(t)\tilde{x}_2(t)$ are finite-energy functions that are square integrable; hence, their moments and Fourier transforms are well defined. Therefore, the integrals in equations (22) and (23) are also well defined. The Melnikov function in equation (21) can be rewritten in the form

$$M(t_0; .) = -D_e + F\ \cos(\Omega t_0 + \tau_0), \tag{24}$$

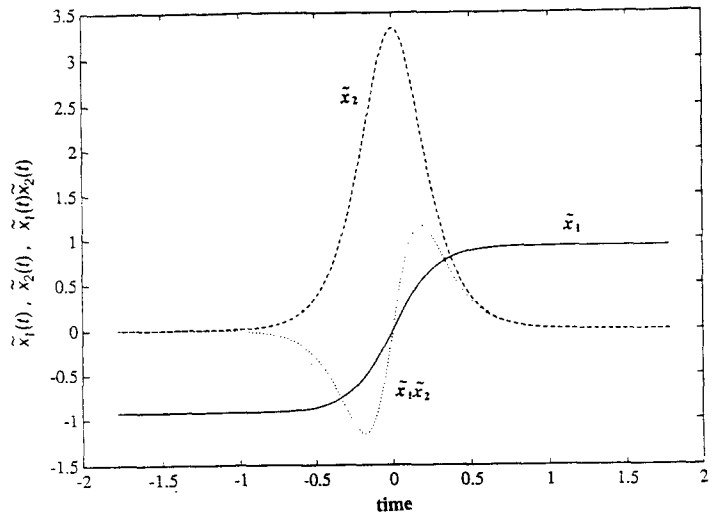


*Fig. 3.* States on the heteroclinic half-orbit.

for some $\tau_0$, where

$$F = \mid f \mid \sqrt{F_c^2 + F_s^2}. \tag{25}$$

If the Melnikov function admits a simple zero, $M(t_0) = 0$ and $\partial M(t_0, .)/\partial t_0 \neq 0$, for some value of $t_0$, then it is known that the stable and unstable manifolds of the Poincaré map have (at least) one transversal intersection (actually an infinity of transversal intersections due to the invariance of the manifolds). For this to occur, it is *necessary* and *sufficient* that

$$\mid D_e \mid = \mid F \cos(\Omega t_0 + \tau_0) \mid \quad \text{and} \quad \mid D_e \mid \neq \mid F \mid \tag{26}$$

for some $t_0$. Equivalently, the Melnikov functions has simple zeros if and only if

$$\mid D_e \mid < F. \tag{27}$$

We note that the inequality (27) is the tightest possible condition, because equation (21) can be transformed into the simple form of equation (24).

It is important to note that the Melnikov criterion as stated in equation (27) is conceptually simple. Note for instance that the effect of the general damping $D(\phi, \dot{\phi})$ is completely and uniquely characterized by the single scalar quantity $D_e$, which is independent of the magnitude, frequency, and phase of the forcing. Indeed, the Melnikov equivalent damping is a function of only the unperturbed Hamiltonian system in equation (7), and hence of the $\alpha_i$, and of the damping coefficients $\mu_i$. In contrast, a steady-state first-order singular perturbation analysis based on the method of multiple scales [23] leads to a modulation equations where there is "interaction" between the damping and forcing parameters [4]. (By "interaction" we mean products of the form $\mu_3\Omega$ or $\mu f$.) This interaction makes the effect of the damping depend on the forcing in a complicated manner, and it becomes sometimes difficult to ascertain the effect of the different damping terms or the effect of damping in general.

We shall show in the next section that the Melnikov-equivalent damping $D_e$ has a very simple structure that allows us to easily ascertain the contribution of different damping terms to the Melnikov function.

## 5. General Analysis of Damping

### 5.1. Damping Models

There are many damping models proposed in the naval architecture literature (e.g., [10, 17–21]). All these models include a linear damping term. Some of these models are

$$D_{LC}(\dot{\phi}) = \mu_1\dot{\phi} + \mu_3\dot{\phi}^3 \tag{28a}$$

$$D_{LQ}(\dot{\phi}) = \mu_1\dot{\phi} + \mu_2 \mid \dot{\phi} \mid \dot{\phi} \tag{28b}$$

$$D_{LQC}(\dot{\phi}) = \mu_1\dot{\phi} + \mu_2 \mid \dot{\phi} \mid \dot{\phi} + \mu_3\dot{\phi}^3 \tag{28c}$$

$$D_{Q}(\phi,\dot{\phi}) = \mu_1\dot{\phi} + m_{11} \mid \phi \mid \dot{\phi} \tag{28d}$$

$$D_{QQ}(\phi,\dot{\phi}) = \mu_1\phi + m_{11} \mid \phi \mid \dot{\phi} + \mu_2 \mid \dot{\phi} \mid \dot{\phi} \tag{28e}$$

$$D_{CC}(\phi,\dot{\phi}) = \mu_1\dot{\phi} + m_{21}\phi^2\dot{\phi} + \mu_3\dot{\phi}^3. \tag{28f}$$

The first two models $D_{LC}(\dot{\phi})$ and $D_{LQ}(\dot{\phi})$ have been studied in [17]. These models as well as $D_{LQC}(\dot{\phi})$ are special cases of the general damping function

$$D(\dot{\phi}) = \sum_{k=1}^{K} \mu_k\dot{\phi} \mid \dot{\phi} \mid^{k-1}, \tag{29}$$

where we require that each individual damping term dissipate energy, and hence, $\mu_k \geq 0$ for all $k$. We note that $D(\dot{\phi})$ is an odd function of $\dot{\phi}$; that is, $D(-\dot{\phi}) = -D(\dot{\phi})$.

### 5.2. Melnikov Damping Coefficients

A closed-form expression for $D_e$ is given by

$$D_e = \sum_{k=1}^{K} \mu_k D_k, \tag{30}$$

where the $D_k$ are positive scalars defined by

$$D_k = \int_{-\infty}^{\infty} \mid \tilde{x}_2(t) \mid^{k+1} \, \mathrm{d}t, \qquad k = 1, 2, ..., K, \tag{31}$$

and shall be referred to as the Melnikov damping coefficients. Since $\tilde{x}_2(t)$ is square integrable, all the $D_k$ are well defined. These coefficients are functions of the $\alpha_i$ only. Moreover, the effect of the different damping terms is simply *additive*, as seen from equation (30).

Next, we discuss different procedures for evaluating the Melnikov damping coefficients $D_k$. An obvious way is to solve for the time history of the heteroclinic half-orbit using an initial-value problem solver, such as a Runge–Kutta method, and to subsequently evaluate the quadratures in equation (31). Alternatively, we can simply use the first integral given in equation (13). Hence, $D_k$ can be written as

$$\begin{aligned} D_k &= \int_{-\phi_S}^{\phi_S} [\psi(\phi)]^k \, \mathrm{d}\phi \\ &= \int_{-\phi_S}^{\phi_S} \left[\alpha_1(\phi_S^2 - \phi^2) + \frac{1}{2}\alpha_3(\phi_S^4 - \phi^4) + \frac{1}{3}\alpha_5(\phi_S^6 - \phi^6)\right]^{k/2} \mathrm{d}\phi. \end{aligned} \tag{32}$$

Evaluating equation (32) is easier than evaluating equation (31). Indeed it can be evaluated with simple quadrature techniques over a finite interval. Evaluating equation (31) requires, on the other hand, the solution of an initial-value problem and the evaluation of a quadrature over an infinite interval. Moreover, equation (32) has the following simple interpretation:

INTERPRETATION OF $D_k$. The coefficient $D_1$ is the area in the $\phi - \psi$ plane under the heteroclinic upper half-orbit, ($\psi \geq 0$), where $\psi(\phi)$ is given by equation (13). Similarly, $D_k$ is the area in the $\phi - \psi$ plane under the curve $[\psi(\phi)]^k$.

More importantly, we note that the Melnikov damping coefficients of even-powered damping terms of the form $\mid \dot{\phi} \mid^{k-1} \dot{\phi}$, where $k$ is even, can be evaluated in closed form, even if the states on the heteroclinic orbit cannot be evaluated in closed form (which is the case when the restoring arm includes quintic and higher-order nonlinearities). The easiest to evaluate is $D_2$:

$$D_2 = \frac{4}{3}\alpha_1 \phi_S^3 + \frac{4}{5}\alpha_3 \phi_S^5 + \frac{4}{7}\alpha_5 \phi_S^7 \tag{33}$$

with $\phi_S$ satisfying equation (12).

### 5.3. Sensitivity Analysis

A sensitivity analysis is often useful to the design engineer. It can determine for example whether the conclusions reached by some analysis are robust to uncertainties in the assumed parameters. A sensitivity analysis can also help the design engineer "get a feel" for the effect of changing some design parameter on some final desired property such as stability.

EXAMPLE (continued). From equation (15), we can show that, for the parameters in equation (5),

$$\frac{d\phi_S}{\phi_S} = \mathbf{S}(\phi_S \mid \omega_0)\frac{d\omega_0}{\omega_0}, \quad \text{where} \quad \mathbf{S}(\phi_S \mid \omega_0) = 1.2467$$

is the relative sensitivity of $\phi_S$ to $\omega_0$. From the value of $\mathbf{S}(\phi_S \mid \omega_0)$ we conclude that increasing $\omega_0$ increases $\phi_S$ (because $\mathbf{S}(\phi_S \mid \omega_0)$ is positive), and that $\phi_S$ is not very sensitive to changes in $\omega_0$ (because $\mathbf{S}(\omega_S \mid \omega_0) \simeq 1$). Were $\mathbf{S}(\phi_S \mid \omega_0) \gg 1$, we would have concluded that $\phi_S$ is very sensitive to variations in $\omega_0$. Similarly, were $\mathbf{S}(\phi_S \mid \omega_0) \ll 1$, we would have concluded that $\phi_S$ is very insensitive to variations in $\omega_0$. All of these conclusions may be helpful to the design engineer. For instance, since the magnitude of $\phi_S$ determines the size of the safe region of the unperturbed system (consider Figure 1a and equation (14)), we conclude that if $d\phi_S/d\alpha_i \geq 0$ then increasing $\alpha_i$ will in general increase the area of the safe region; a desirable effect.

Here, we consider the issue of characterizing the so-called sensitivity derivatives of which $d\phi_S/d\alpha_1$ is an example. One advantage of using the first integral of motion in equation (13) in that the sensitivity of the Melnikov equivalent damping to variations in the parameters characterizing the ship (not including the damping coefficients $\mu_i$ themselves) can be easily addressed. For instance, the sensitivity of $D_e$ to variations in the natural frequency $\omega_0 = \sqrt{\alpha_1}$ of the ship can be determined from $dD_E/d\alpha_1 = \Sigma_i \mu_i dD_i/d\alpha_1$. If the sensitivity derivatives can be shown to be all positive and if all $\mu_i \geq 0$, then $dD_e/d\alpha_1 > 0$, and hence, *an increase in the natural frequency of the ship increases $D_e$, thus suggesting more energy dissipation.*

We begin by determining the sensitivity of $D_2$ to variations in any parameter $\alpha_i$. Differentiation equation (33) with respect to $\alpha_i$ and making use of equation (15), we obtain

$$\frac{dD_2}{d\alpha_i} = -\frac{4[\alpha_1\phi_S^2 + \alpha_3\phi_S^4 + \alpha_5\phi_S^6]\phi_S^i}{\alpha_1 + 3\alpha_3\phi_S^3 + 5\alpha_5\phi_S^5} + \frac{4}{i+2}\phi_S^{i+2} = \frac{4}{i+2}\phi_S^{i+2} \tag{34}$$

where the first term is zero on account of equation (11). Since $\phi_S > 0$, this derivative is positive and hence, if $\mu_s > 0$, *increasing $\alpha_i$ will increase the stabilizing effect of the quadratic damping term.* Moreover, we can show that equation (34) can be written in the form

$$\frac{dD_2}{D_2} = \mathrm{S}(D_2 \mid \alpha_i)\left|\frac{d\alpha_i}{\alpha_i}\right|, \quad \text{where} \quad \mathrm{S}(D_2 \mid \alpha_i) = \frac{4 \mid \alpha_i \mid \phi_S^{i+2}}{(i+2)D_2}$$

represents the realtive sensitivity of $D_2$ to $\alpha_i$.

EXAMPLE (continued). For the parameters in equation (5), $D_2 = 10.7373$, and hence, $\mathrm{S}(D_2 \mid \alpha_i) = 2.7316$ and $\mathrm{S}(D_2 \mid \alpha_3) = 1.963$. Thus, *$D_2$ is more sensitive to variations in $\alpha_1$ than to variations in $\alpha_3$.*

For the general system shown in equation (16), $D_2$ and its sensitivity derivatives are given by, respectively,

$$D_2 = 4\sum_{i=1}^{N}\frac{\alpha_{i+2}}{i+2}\phi_S^{i+2} \quad \text{and} \quad \frac{dD_2}{d\alpha_i} = \frac{4}{i+2}\phi_S^{i+2} > 0. \tag{35}$$

We note that $dD_2/d\alpha_i$ is always positive, which implies a stabilizing effect as far as the damping is concerned. (The effect of varying $\alpha_i$ on $F_c$ and $F_s$ is yet to be determined.) It is of interest to determine whether $dD_k/d\alpha_i \geq 0$ for all $k$ and $i$. We use Leibnitz's rule to differentiate the general expression in equation (32) with respect to $\alpha_i$, where $\psi(\phi)$ is given in equation (17). After some symbolic manipulation, we obtain

$$\begin{aligned}\frac{dD_k}{d\alpha_i} &= \left[4\sum_{j\ \text{even}}\frac{\alpha_j}{j+1}\phi_S^{j+1}\right]^{k/2}\cdot\frac{d\phi_S}{d\alpha_i} \\ &\quad + \frac{k}{i+1}\int_{-\phi_S}^{\phi_S}[\Psi(\phi_S) - \Psi(\phi)]^{k/2-1}\cdot(\phi_S^{i+1} - \phi^{i+1})\,d\phi\end{aligned} \tag{36}$$

which can be expressed in closed form if $k$ is even. Often, all we need to determine is the sign of these derivatives.

As an example, we assume that $\alpha_j = 0$ for even values of $j$. In this case, the first term in equation (36) vanishes, and if $\alpha_i \geq 0$, then $dD_k/d\alpha_i \geq 0$. Indeed, since $\mid \phi \mid < \phi_S$ on the heteroclinic orbit, and since $i$ and $j$ are restricted to be odd numbers, the integrand in equation (36) is positive (or complex which is not acceptable). The generality of this conclusion is a curious fact. It means that if $\alpha_i = 0$ for *$i$ even* (and $\mu_i \geq 0$) then an increase in $\alpha_i$ increases $D_e$, thus suggesting more energy dissipation. Similarly, since $D_1$ represents the area of the safe region of the unperturbed system, the sensitivity derivative $dD_1/d\alpha_i$ tells about the variation of this area with any parameter $\alpha_i$. We note finally that equation (35) is a special case of equation (36) obtained with $k = 2$, and it is positive irrespective of the signs of the $\alpha_i$.

### 5.4. Effect of Different Damping Terms

To ascertain ther relative importance of the different damping terms, we note that equation (30) can be written in the form

$$D_e = \mu_1 D_1 (1 + \nu_2 + \nu_3 + ...) \tag{37}$$

where

$$\nu_k = \frac{\mu_k D_k}{\mu_1 D_1} \tag{38}$$

represents the importance of the $k^{\text{th}}$ damping term relative to the linear damping term. Here, we took the linear damping term as a basis for comparison. Of course, one can choose the quadratic (or any other) damping term as a basis for comparison, if that term is the dominant one.

When $\psi_{\max}$, the maximum roll velocity on the heteroclinic orbit, is either too large or too small, the relative importance of every damping term becomes easier to ascertain. In particular,

$$\text{If } \psi_{\max} < 1 \Rightarrow D_1 > D_2 > D_3 > ... \tag{39}$$

To prove equation (39), we note that on the heteroclinic upper half-orbit, $\sigma(\phi) = (\psi(\phi)/\psi_{\max}) \leq 1$, and hence if $k < \ell$, then

$$\frac{D_k}{\psi_{\max}^k} - \frac{D_\ell}{\psi_{\max}^\ell} = \int_{-\phi_S}^{\phi_S} [\sigma^k(\phi) - \sigma^\ell(\phi)]\, \mathrm{d}\phi > 0. \tag{40}$$

Therefore,

$$D_k > \psi_{\max}^{k-\ell} D_\ell \tag{41}$$

and with $k < \ell$ and $\psi_{\max} < 1$, equation (38) results. Now if all the $\mu_i$ are equal, then

$$1 = \nu_1 > \nu_2 > \nu_3 > ... \tag{42}$$

from which we conclude that if any two damping terms $\mu_i \mid \dot{\phi} \mid \dot{\phi}^{i-1}$ and $\mu_j \mid \dot{\phi} \mid \dot{\phi}^{j-1}$, with $i < j$, have equal damping coefficients, $\mu_i = \mu_j$, then *the lower-order damping term (the $i^{th}$ term) is more effective in stabilizing the ship.*

For a large enough $\psi_{\max}$, we expact the converse relation of equation (39) to hold; namely, we expect that $D_1 < D_2 < D_3 < ....$ We do not as yet have a proof for this conjecture.

## 6. Equivalence of Quadratic and Cubic Damping

The linear-plus-quadratic damping (LPQD) model shown in equation (28b) is often used to model the drag experienced by a body moving through a fluid. In naval architecture, this model is used to model the dissipation due to bilge keels, antiroll fins, and other appendages on the ship hull as they move through water. In the context of perturbation and bifurcation analyses, the LPQD model is not very appealing, because it is only once differentiable. For instance, it is not possible to carry out a second- or third-order perturbation analysis with an equation having this damping model. Therefore, the LPQD model is often approximated with the linear-plus-cubic damping (LPCD) model shown in equation (28a), which is infinitely differentiable.

Traditionally, the damping coefficients $\mu_1$, $\mu_2$, ..., are determined by curve-fitting experimental free-decay data. One may therefore jump to the conclusion that two damping models are "equivalent" if they yield the same free-decay behavior. Two damping models with identical free-decay behavior can have, as we will illustrate later in this section, quite different forced-oscillation behavior. Here, we explore under what conditions $D_{LC}(\dot{\phi})$ and $D_{LQ}(\dot{\phi})$ defined in equation (28a–b) also exhibit identical transient and steady-state forced-oscillation behavior in addition to exhibiting identical free-decay behavior.

Following [17], we seek an approximation of the quadratic terms in $D_{LQ}(\dot{\phi})$ in terms of the first two odd powers of $\dot{\phi}$ as follows:

$$\dot{\phi} \mid \dot{\phi} \simeq \beta_1 \dot{\phi}_c \dot{\phi} + \beta_3 \frac{\dot{\phi}^3}{\dot{\phi}_c}. \tag{43}$$

This approximation is made in the least-squares sense so that the error

$$E = \int_{-\dot{\phi}_c}^{\dot{\phi}_c} \left[ \beta_1 \dot{\phi}_c \dot{\phi} + \beta_3 \frac{\dot{\phi}^3}{\dot{\phi}_c} - \mid \dot{\phi} \mid \dot{\phi} \right]^2 \mathrm{d}\dot{\phi} \tag{44}$$

is minimized over all possible values of $\beta_1$ and $\beta_3$, where $\dot{\phi}_c$ represents the range of $\dot{\phi}$ over which the approximation is presumed to hold. Requiring $E$ to be stationary with respect to $\beta_1$ and $\beta_3$ results in [17]

$$\beta_1 = \frac{5}{16}, \quad \beta_3 = \frac{35}{48}, \quad \text{and} \quad E = \frac{\dot{\phi}_c^3}{96}. \tag{45}$$

Then, the two damping models $D_{LQ}(\dot{\phi})$ and $D_{LC}(\dot{\phi})$ are close over the interval $\dot{\phi} \in [-\dot{\phi}_c, \dot{\phi}_c]$ in the least-squares sense if

$$\mu_1 + \beta_1 \dot{\phi}_c \mu_2 = \hat{\mu}_1 \quad \text{and} \quad \frac{\beta_3}{\dot{\phi}_c} \mu_2 = \hat{\mu}_3, \tag{46}$$

where $\mu_1$ and $\mu_2$ determine $D_{LQ}(\dot{\phi})$ and $\hat{\mu}_1$ and $\hat{\mu}_3$ determine $D_{LC}(\dot{\phi})$.

There remains the issue of how to choose $\dot{\phi}_c$, which determines the domain of least squares matching. For instance, if the LPCD model $D_{LC}(\dot{\phi})$ was given, and we were seeking an equivalent LPQD model $D_{LQ}(\dot{\phi})$, it is possible that equation (46) would yield a negative value for $\mu_1$, especially if $\dot{\phi}_c$ is large. A negative $\mu_1$ is not acceptable on physical grounds. Fortunately, it is usually the case that we seek to approximate $D_{LQ}(\dot{\phi})$ by $D_{LC}(\dot{\phi})$, and in this case, $\hat{\mu}_1$ and $\hat{\mu}_3$ are always positive provided that $\mu_1$ and $\mu_2$ are positive (see equation (46)). The positiveness of the damping coefficients is not the only consideration determining whether $\dot{\phi}_c$ is acceptable or not. If $\dot{\phi}_c$ is very small, the approximation in equation (43) may not be valid over the range of dynamics that is relevant to the ship stability. We expect $\omega_0$ or $\psi_{\max}$ to give us crude yet physically meaningful approximations of this range. Another consideration is the goodness of the least-squares fit, as measured by the error E in equation (45), which deteriorates as $\dot{\phi}_c$ becomes too large.

To illustrate the importance of choosing a not-too-small value of $\dot{\phi}_c$, we consider some of the damping models used in [17] to characterize the unbiased low-freeboard model of [2] (see equation (5)). The LPQD model

$$D_{LQ}(\dot{\phi}) = 2 \times 0.063\dot{\phi} + 0.148 \mid \dot{\phi} \mid \dot{\phi} \tag{47}$$

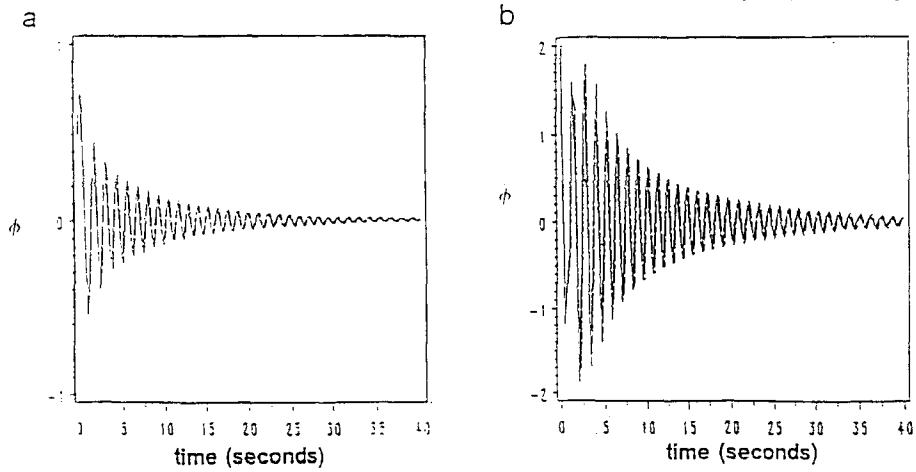


*Fig. 4.* Free-decay response for the initial conditions $\phi = 0.5$ and $\dot{\phi} = 2.0$: (a) roll amplitude and (b) roll velocity. Solid lines correspond to the LPCD model in equation (48) and broken lines correspond to the LPQD model in equation (47).

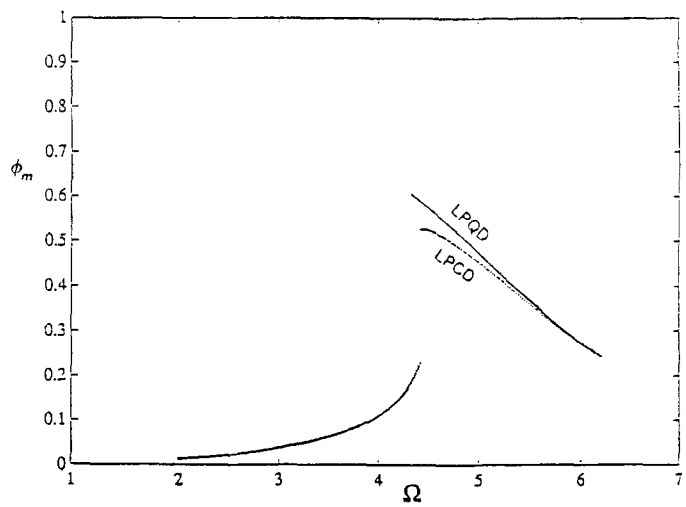


*Fig. 5.* Frequency-response curves for $s_m = 0.1$ of the LPCD and LPQD damping models matched with $\dot{\phi}_c = 1$.

can be approximated in the least squares sense with $\dot{\phi}_c = 1$ by the LPCD model [17]

$$\dot{\phi}_c = 1 \Rightarrow D_{LC}(\dot{\phi}) = 2 \times 0.086\dot{\phi} + 0.1080\dot{\phi}^3. \tag{48}$$

We show in Figure 4 the free-decay curves corresponding to the models. They are almost the same. The frequency-response curves of the two models are quite different as it is shown in Figure 5. In Figure 5, $\phi_m$ represents the maximum roll amplitude. Similarly, the two models yield different Melnikov predictions and different basins of safety as shown in Figures 6 and 7, respectively. These basins, as well as subsequent ones, are computed by integrating equation (6) for 20 forcing periods starting from a $400 \times 400$ grid of initial conditions, and checking ten times every period whether the states are inside or outside the box formed by $\phi \in [-1.2, 1.2]$ and $\dot{\phi} \in [-10, 10]$. Integrating from initial conditions in the black (capsize) region leads to states outside the box.

To overcome the problem of choosing a too-small $\dot{\phi}_c$, Dalzell [17] proposed an iterative procedure in which one assumes some $\dot{\phi}_c$ and then computes the maximum roll velocity under

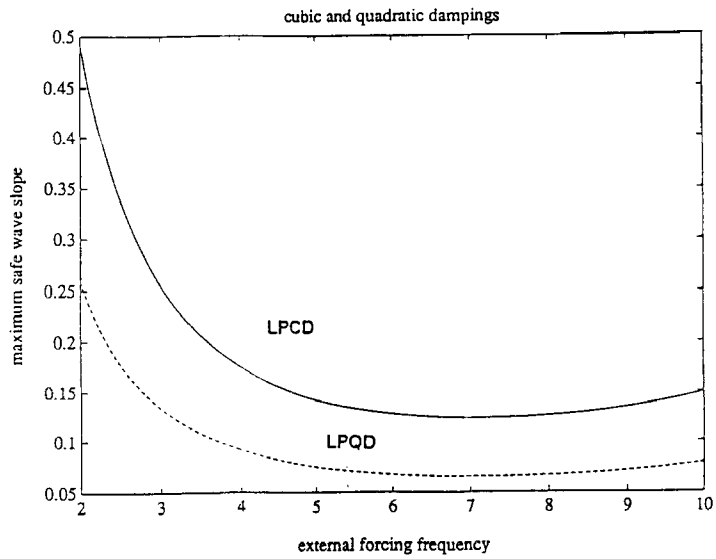


*Fig. 6.* Maximum safe wave slope for the two damping models with $\dot{\phi}_c = 1$.

a particular forcing condition. If this maximum roll velocity is larger than the assumed $\dot{\phi}_c$, then $\dot{\phi}_c$ is increased, and the procedure is repeated. Unfortunately, this procedure has to be repeated for every forcing condition and does not guarantee the same Melnikov predictions.

Here, we ask whether a judicious choice of $\dot{\phi}_c$ can yield the same Melnikov predictions. Since in the Melnikov analysis, the effect of the damping is independent of the forcing, we have the same Melnikov predictions if the two models have the same value of the Melnikov equivalent damping: $D_e^{LQ} = D_e^{LQ}$. This requires that, in addition to the conditions in equation (46), the following condition holds:

$$\mu_1 D_1 + \mu_2 D_2 = \hat{\mu}_1 D_1 + \hat{\mu}_3 D_3. \tag{49}$$

Since $\dot{\phi}_c$ has not been specified yet, equations (46) and (49) can be thought of as consisting of three equations in the three unknowns $\hat{\mu}_1$, $\hat{\mu}_3$, and $\dot{\phi}_c$. These equations admit a real solution if and only if the condition

$$D_2^2 - 4(\beta_1 D_1)(\beta_3 D) \leq 0 \tag{50}$$

holds. If equation (50) is satisfied, we obtain the real quantity

$$\dot{\phi}_c = \frac{D_2 \pm \sqrt{D_2^2 - 4(\beta_1 D_1)(\beta_3 D_3)}}{2\beta_1 D_1}. \tag{51}$$

We note that equations (50) and (51) are independent of the damping coefficients $\mu_i$ and the forcing, and are function of the $\alpha_i$ only. The value of $\dot{\phi}_c$ defined in equation (51) may still be unacceptable, and its acceptability has to be carefully examined.

EXAMPLE (continued). For the ship in equation (5), we have $D_1 = 4.0497$, $D_2 = 10.7373$, and $D_3 = 30.5851$. Therefore, condition (50) is satisfied and there are two values, $\dot{\phi}_c = 3.6305$ rad/second and $\dot{\phi}_c = 4.8540$ rad/second, for which the LPQD and LPCD damping models are equivalent in the sense of Melnikov. Both of these values of $\dot{\phi}_c$ are between $\psi_{\max} = 3.334$

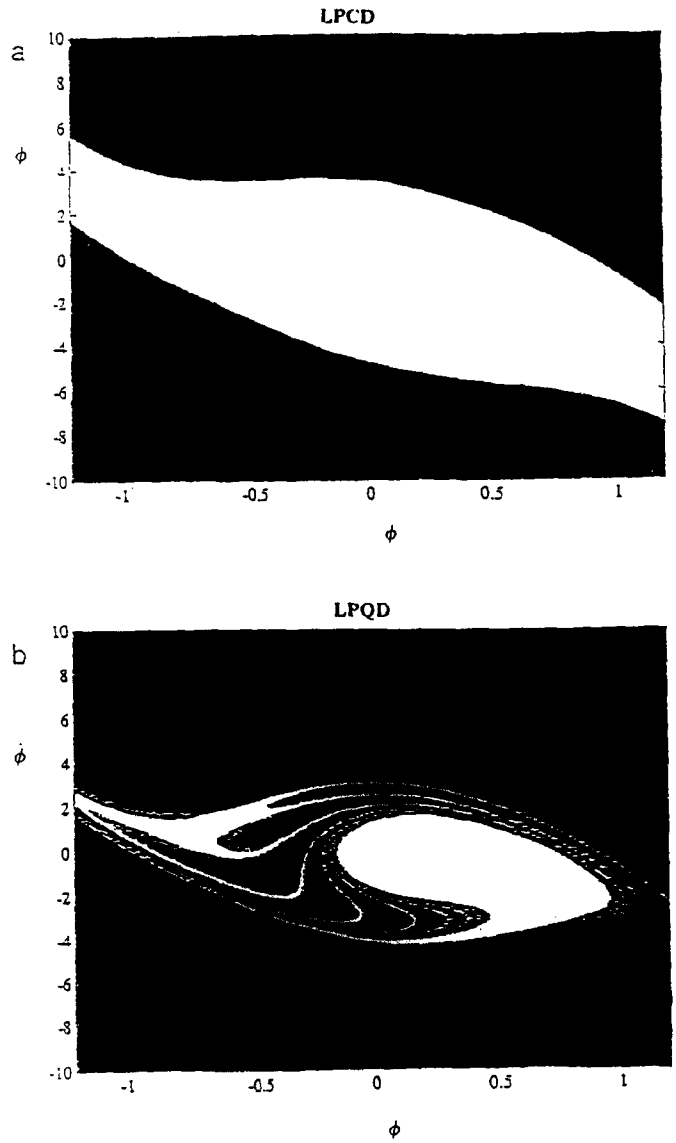


*Fig. 7.* Basins of safe and capsize regions for a model with quintic restoring terms at $s_m = 0.24$, $\Omega = 0.7\omega_0$, and $\dot{\phi}_c = 1$: (a) LPCD model and (b) LPQD model.

and the natural frequency of the ship $\omega_0 = 5.278$ rad/sec. Hence, we expect that both of these values of $\dot{\phi}_c$, not to be too small.

In Figure 8, we compare the LPQD model $D_{LQ}(\dot{\phi})$ with the approximate LPCD models obtained with $\dot{\phi}_c = 1, 3.6305$, and 4.8540 rad/sec. For $\dot{\phi}_c = 3.6305$, we obtain

$$D_{LC}(\dot{\phi}) = 2 \times 0.147\dot{\phi} + 0.02970\dot{\phi}^3. \tag{52}$$

In Figures 9–11, we show the frequency-response curves and the basins of safety corresponding to the two models. Figure 10 (Figure 11) corresponds to a level of forcing that is lower (higher) than the level at which the heteroclinic bifurcation occurs. We note that the obtained results are almost indistinguishable unlike those reported in Figures 5–7 obtained with $\dot{\phi}_c = 1$. Hence the two models shown in Figure 8 have the same steady-state and transient forced responses.

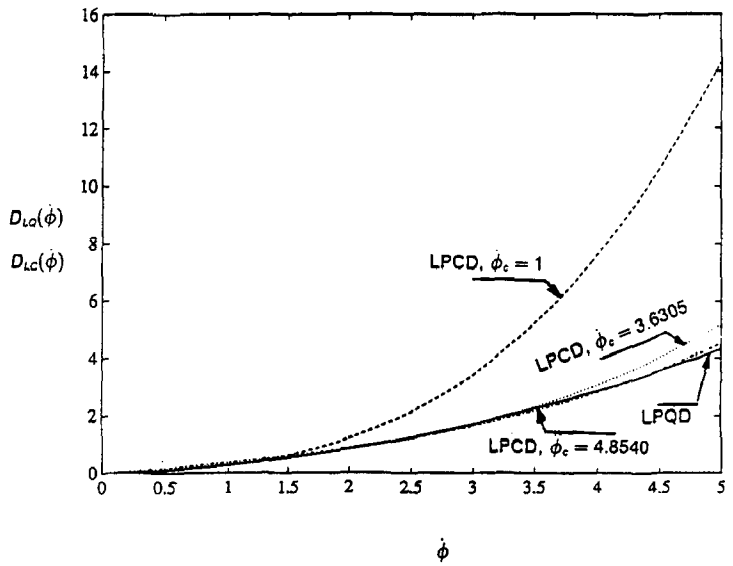


*Fig. 8.* $D_{LQ}(\dot{\phi})$ in equation (47) and its least-squares approximations obtained with $\dot{\phi}_c = 1$, 3.6305 and 4.8540.

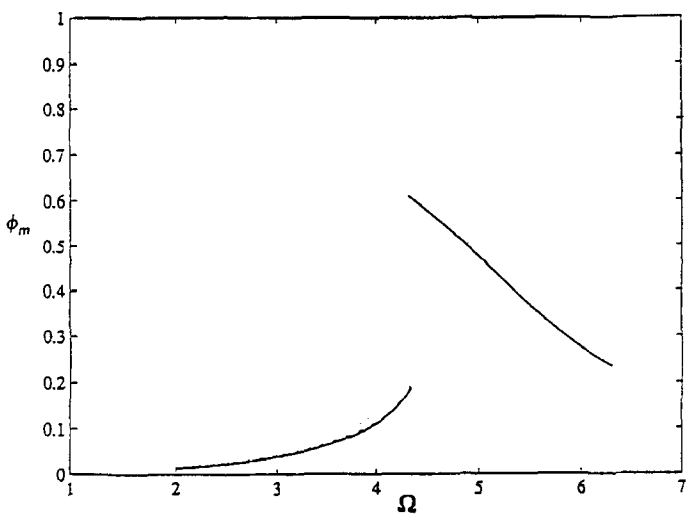


*Fig. 9.* Frequency-response curves when $s_m = 0.1$ for the LPCD and LPQD models obtained with $\dot{\phi}_c = 3.6305$ (see equations (47) and (52)).

For $\dot{\phi}_c = 4.8540$ rad/second,

$$D_{LC}(\dot{\phi}) = 2 \times 0.1750\dot{\phi} + 0.02220\dot{\phi}^3. \tag{53}$$

In Figures 12–14, we show the frequency-response curves and the basins of safety before and after the heteroclinic bifurcation for the two damping models. These basins are again very similar, thus suggesting that the *transient* responses as well as the *steady-state* responses corresponding to the two damping models are very similar.

Finally, we use equation (46) to express $D_e^{LC}$ given by equation (30) as a function of $\dot{\phi}_c$:

$$D_e^{LC}(\dot{\phi}_c) = \mu_1 D_1 + \mu_2\beta_1 D_1\dot{\phi}_c + \frac{\mu_2\beta_3 D_3}{\dot{\phi}_c}. \tag{54}$$

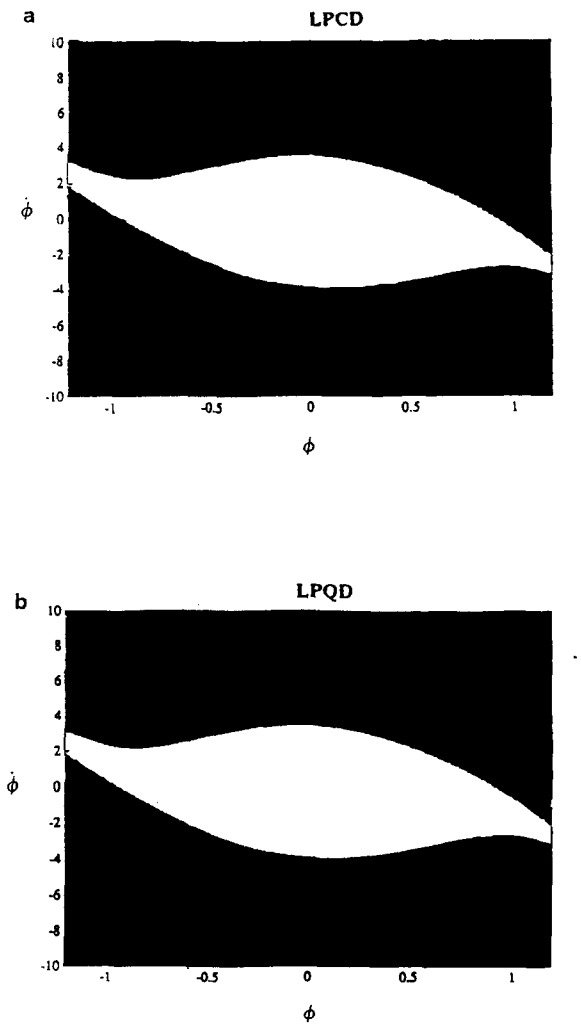


*Fig. 10.* Basins of safe and capsize regions for the LPCD and LPQD models obtained with $\dot{\phi}_c = 3.6305$. Forcing is specified by $s_m = 0.1$ and $\Omega = 0.7\omega_0$.

Clearly, this function approaches infinity as $\dot{\phi}_c \to 0$, or as $\dot{\phi}_c \to \infty$, thus illustrating the importance of avoiding choices of $\dot{\phi}_c$ that are too small or too large. We show in Figure 15 variation of the ratio

$$\frac{D_e^{LC}(\dot{\phi}_c)}{D_e^{LQ}}$$

with $\dot{\phi}_c$ for the example discussed above. For the values of $\dot{\phi}_c$ computed in equation (51), this ratio takes a value of one. Note that values of $\dot{\phi}_c$ between the two values given by equation (51) should give almost the same Melnikov predictions and are hence acceptable, but other

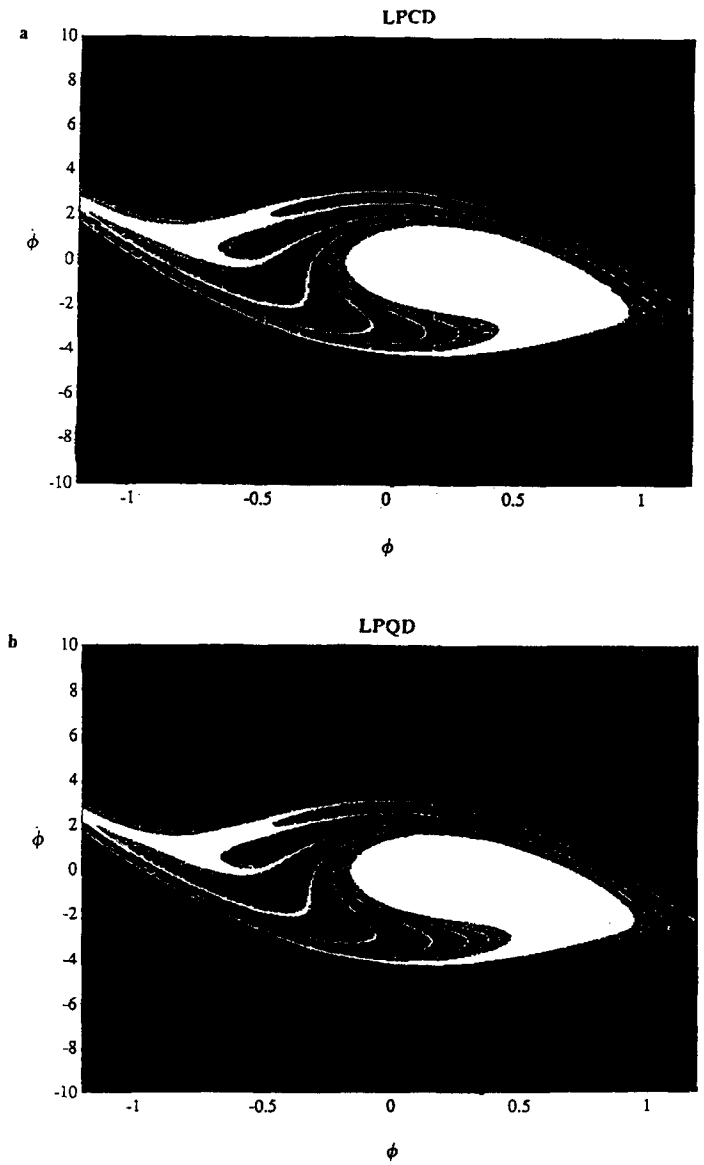


*Fig. 11.* Basins of safe and capsize regions for the LPCD and LPQD models obtained with $\dot{\phi}_c = 4.8540$. Forcing is specified by $s_m = 0.24$ and $\Omega = 0.7\omega_0$.

values will not. Any choice $\psi_{\max} \leq \dot{\phi}_c \leq \omega_0$ is therefore reasonable, but only in hindsight. The behavior in Figure 15 may be particular to the ship of [2] for which the minimum of $D_e^{LC}(\dot{\phi}_c)$ is very close and just below the value of $D_e^{LQ}$. We cannot expect this to hold in general.

If the minimum of $D_e^{LC}(\dot{\phi}_c)$ is smaller than $D_e^{LQ}$, then as we showed in equations (49)–(51), these two quantities can be made equal by choosing $\dot{\phi}_c$ according to equation (51). If, however, $D_e^{LC}(\dot{\phi}_c) > D_e^{LQ}$ for all $\dot{\phi}_c$, then equation (50) is not satisfied, and the two damping models can never yield the same Melnikov predictions. In this case, we seek the value fo $\dot{\phi}_c$ that minimize $D_e^{LC}(\dot{\phi}_c)$ in equation (54), since this choice yields the best possible

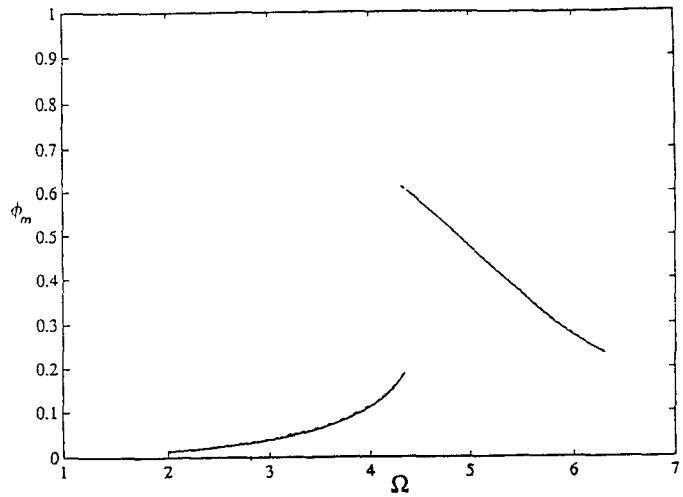


*Fig. 12.* Frequency-response curves when $s_m = 0.1$ for the LPCD and LPQD models obtained with $\dot{\phi}_c = 4.8540$.

approximation to $D_e^{LQ}$. This is achieved by solving for a value of $\dot{\phi}_c$ that satisfies the condition $dD_e^{LC}(\dot{\phi}_c)/d\dot{\phi}_c = 0$ and $d^2D_e^{LC}(\dot{\phi}_c)/d\dot{\phi}_c^2 > 0$. The solution is given by

$$\dot{\phi}_c = \sqrt{\frac{\beta_3 D_3}{\beta_1 D_1}} \quad \text{and} \quad D_e^{LC} = \mu_1 D_1 + 2\mu_2\sqrt{(\beta_1 D_1)(\beta_3 D_3)} \tag{55}$$

where $\dot{\phi}_c$ is independent of $\mu_1$, $\mu_2$, $f$, and $\Omega$.

## 7. Conclusions

In this paper, we conducted a detailed Melnikov analysis for the roll motions of a ship in regular beam seas for a variety of damping models. We assessed the effect of the different damping terms on the Melnikov function and hence on the immunity of the ship to capsizing. Furthermore, these effects are additive. Our approach for evaluating the Melnikov damping coefficients is based on evaluating the first integral of motion. Many simple conclusions and closed-form expressions can be obtained even if the time histories of the states on the heteroclinic orbits cannot be evaluated in closed form. As an application of our formulas, we derived a condition under which the linear-plus-cubic damping model approximates well the linear-plus-quadratic damping model in a least-squares sense, and, at the same time, yields the same Melnikov predictions for all wave slopes and wave encounter frequencies. Simulations have shown that if this condition holds, then the two models not only have the same free-decay responses, but also have the same (or very similar) forced steady-state and transient behaviors. Simulations have also indicated that the scaling used in the Melnikov analysis is appropriate for the example considered.

## Acknowledgements

This work was supported by the Office of Naval Research under Grant No. N00014-90-J-1149. We also thank the reviewers for their constructive suggestions and criticisms.

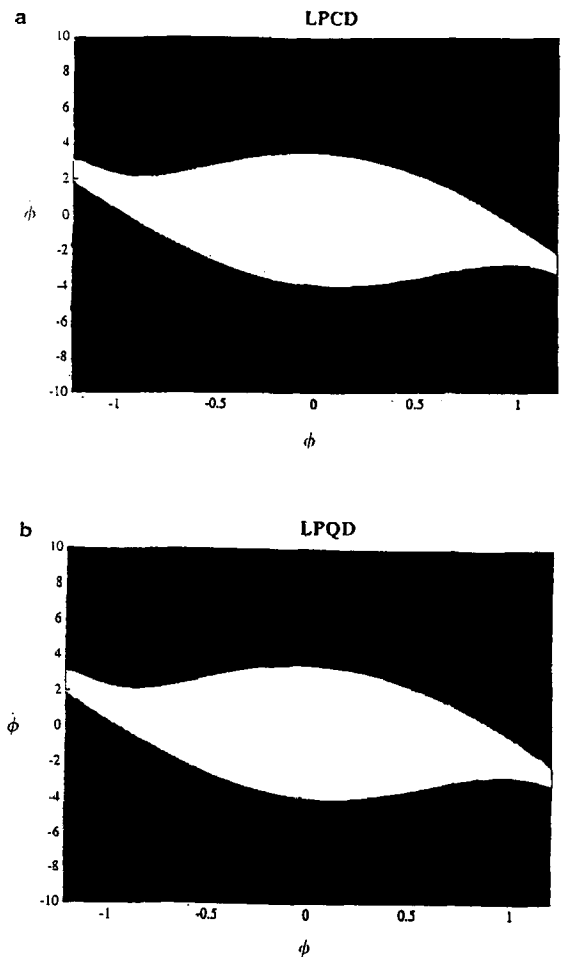


*Fig. 13.* Basins of safe and capsize regions for the LPCD and LPQD models shown above obtained with $\dot{\phi}_c = 4.8540$. Forcing is specified by $s_m = 0.1$ and $\Omega = 0.7\omega_0$.

## References

1. The papers of William Froude, The Institution of Naval Architects, London, 1955.
2. Wright, J. H. G. and Marshfield, W. B., 'Ship roll response and capsize behaviour in beam seas', *Transactions of the Royal Institute of Naval Architects* **122**, 1979, 129–148.
3. Nayfeh, A. H. and Khdeir, A. A., 'Nonlinear rolling of ships in regular beam seas', *International Shipbuilding Progress* **33**, 1986, 40–49.
4. Nayfeh, A. H. and Sanchez, N. E., 'Chaos and dynamic instabilities of the rolling motion of ships', *Proceedings of the 17th Symposium on Naval Hydrodynamics*, The Hague, The Netherlands, August–September 1988.
5. Nayfeh, A. H. and Sanchez, N. E., 'Stability and complicated rolling responses of ships in regular beam seas', *International Shipbuilding Progress* **37**, 1990, 331–352.
6. Virgin, L., 'The nonlinear rolling response of a vessel including chaotic motions leading to capsize in regular seas', *Applied Ocean Research* **9**, 1987, 89–95.

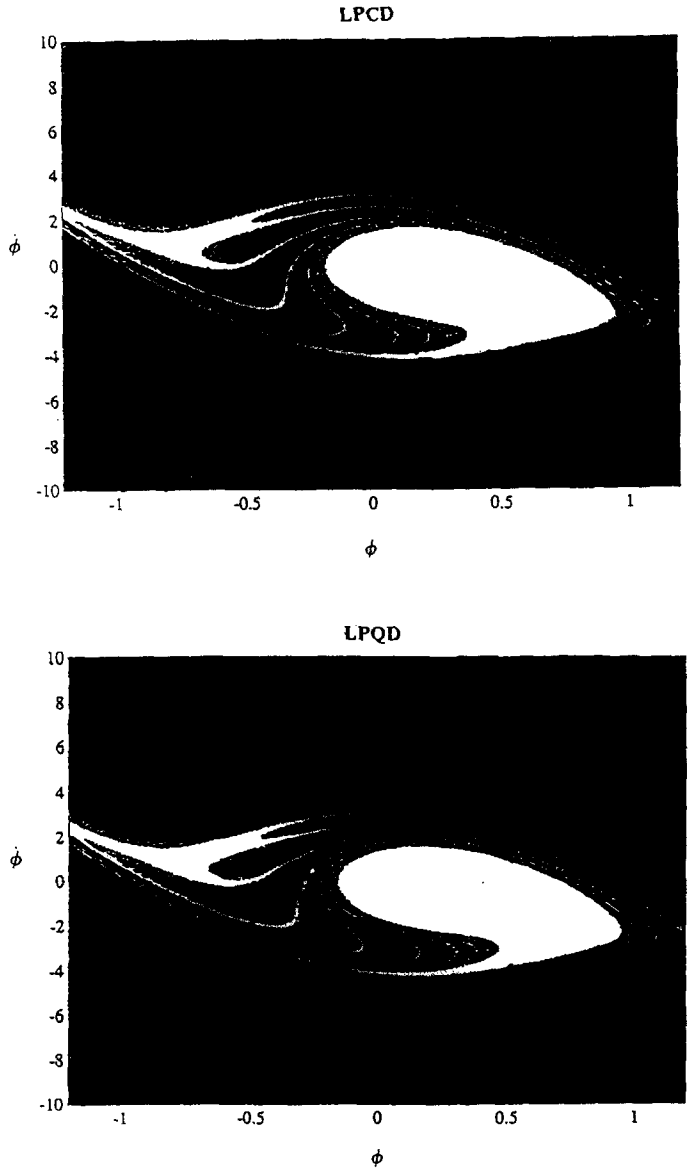


*Fig. 14.* Basins of safe and capsize regions for the LPCD and LPQD models obtained with $\dot{\phi}_c = 4.8540$. Forcing is specified by $s_m = 0.24$ and $\Omega = 0.7\omega_0$.


7. Thompson, J. M. T., Rainey, R. C. T., and Soliman, M. S., 'Ship stability criteria based on chaotic transients from incursive fractals', *Philosophical Transactions of the Royal Society of London* **332**, 1990, 149–167.
8. Soliman, M. S., 'An analysis of ship stability based on transient motions', *Proceedings of the Fourth International Conference on the Stability of Ships and Ocean Vehicles*, Naples, Italy, September 1990.
9. Falzarano, J. M. and Troesch, A. W., 'Application of modern geometric methods for dynamical systems to the problem of vessel capsizing with water-on-deck', *Proceedings of the Fourth International Conference on the Stability of Ships and Ocean Vehicles*, Naples, Italy, September 1990.
10. Falzarano, J. M., 'Predicting complicated dynamics leading to vessel capsizing', Ph.D. Thesis, Department of Naval Architecture and Marine Engineering, University of Michigan, Ann Arbor, MI, 1990.
11. Falzarano, J. M., Shaw, S. W., and Troesh, A. W., 'Application of global methods for analyzing dynamical systems to ships rolling motion and capsizing', *International Journal of Bifurcation and Chaos* **2**, 1992, 101–115.

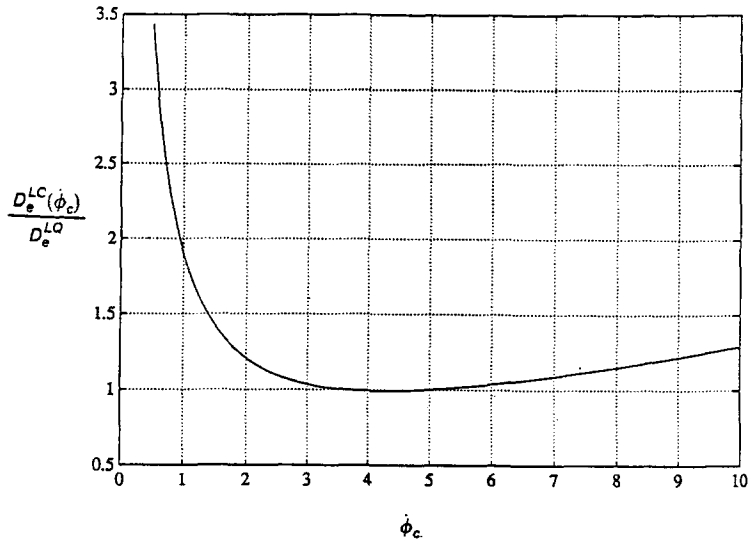


*Fig. 15.* Variation of $D_e^{LC}(\dot{\phi}_c)/D_e^{LQ}$ with $\dot{\phi}_c$.


12. Guckenheimer, J. and Holmes, P., *Nonlinear Oscillations, Dynamical Systems, and Bifurcations of Vector Fields*, Springer-Verlag, New York, 1983.
13. Melnikov, V. K., 'On the stability of the center for time-periodic perturbations', *Transactions of the Moscow Mathematical Society* **12**, 1963, 11–57.
14. Wiggins, S., *Introduction to Applied Nonlinear Dynamical Systems and Chaos*, Springer-Verlag, New York, 1990.
15. Salam, F. M. A., 'The Melnikov technique for highly dissipative systems', *SIAM Journal of Applied Mathematics* **47**, 1987, 232–243.
16. Kreider, M., 'A numerical investigation of the global stability of ship roll: Invariant manifolds, Melnikov's method, and transient basins', M. S. Thesis, Department of Engineering Science and Mechanics, Virginia Polytechnic Institute and State University, Blacksburg, VA, 1992.
17. Dalzell, J. F., 'A note on the form of ship roll damping', *Journal of Ship Research* **22**, 1978, 178–185.
18. Cardo, A., Francescutto, A., and Nabergoj, R., 'On damping models in free and forced rolling motion', *Ocean Engineering* **9**, 1982, 171–179.
19. Mathisen, J. B. and Price, W. G., 'Estimation of ship roll damping coefficients', *Transactions of the Royal Institution of Naval Architects* **127**, 1984, 295–307.
20. Bass, D. W. and Haddara, M. R., 'Nonlinear models of ship roll damping', *International Shipbuilding Progress* **35**, 1988, 5–24.
21. Haddara, M. R. and Bennett, P., 'A study of the angle dependence of roll damping moment', *Ocean Engineering* **16**, 1989, 411–427.
22. Lugovsky, V. V., *Nonlinear Problems of Ship Seaworthiness*, Sudostroenine Publishers, Leningrad, 1966, in Russian.
23. Nayfeh, A. H., *Introduction to Perturbation Techniques*, John Wiley & Sons, New York, 1981.
24. Nayfeh, A. H., 'On the undesirable roll characteristics of ships in regular seas', *Journal of Ship Research* **32**, 1988, 92–100.
25. Hind, J. A., *Stability and Trim of Fishing Vessels*, Fishing New Books Ltd., England, 1982.
26. Parker, T. S. and Chua, L. O., *Practical Numerical Algorithms for Chaotic Systems*, Springer-Verlag, New York, 1989.
27. Li, G. X. and Moon, F. C., 'Criteria for chaos of a three-well potential oscillator with homoclinic and heteroclinic orbits', *Journal of Sound and Vibration* **136**, 1990, 17–34.